Molecular BioSystems

Accepted Manuscript

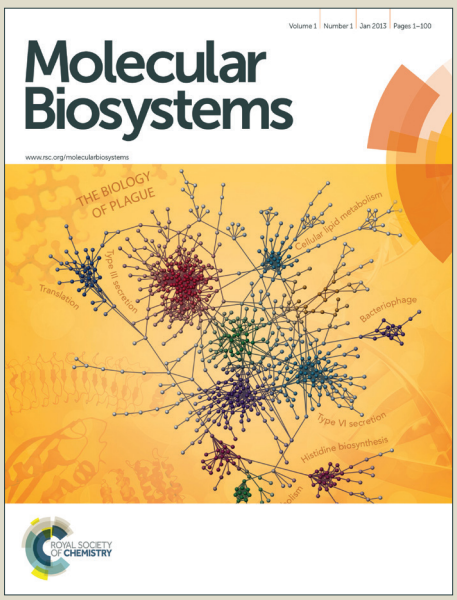

ROYAL SOCIETY OF CHEMISTRY

www.rsc.org/molecularbiosystems

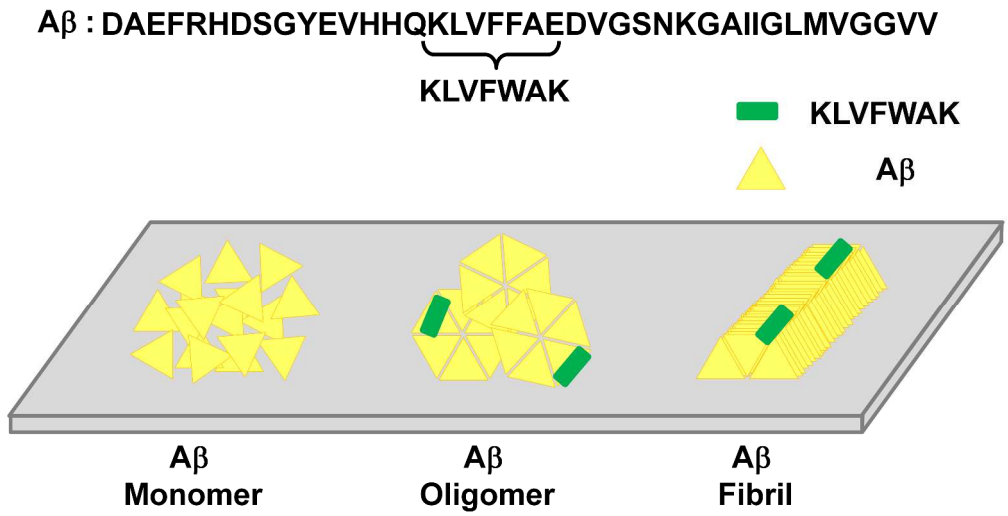

A non-self-aggregating peptide ligand for β-amyloid aggregates created by simple point mutation of an β-amyloid-derived segment
1434x745mm (96 x 96 DPI)

Engineering of a peptide probe for β-amyloid aggregates

Edwin Aoraha, Jason Candreva and Jin Ryoun Kim*

Othmer-Jacobs Department of Chemical and Biomolecular Engineering

New York University

6 MetroTech Center, Brooklyn, NY 11201 (USA)

Fax: (+1) 718-260-3125

E-mail: jin.kim@nyu.edu

***Corresponding author**: Prof. Jin Ryoun Kim, Othmer-Jacobs Department of Chemical and Biomolecular Engineering, New York University, 6 MetroTech Center, Brooklyn, NY 11201, USA. Tel: 1-718-260-3719. Fax: 1-718-260-3125. Email: jin.kim@nyu.edu

Running title: A peptide probe for β-amyloid aggregates

Keywords: amyloid aggregation; β-amyloid; protein engineering; peptide probe

Abbreviations used:

Aβ, β-amyloid; AD, Alzheimer's disease; HCD, hydrophobic central domain; SEC, size exclusion chromatography; DLS, dynamic light scattering; kcps, kilo counts per second; CD, circular dichroism; TEM, transmission electron microscopy; LMW, low molecular weight; FITC, fluorescein iso-thiocyanate; ThT, Thioflavin T; PET, positron emission tomography; PBSA, phosphate-buffered saline with azide; HFIP, hexafluoroisopropanol; PBA, phosphate buffer with azide; DMSO, dimethyl sulfoxide; PAGE, polyacrylamide gel electrophoresis

ABSTRACT

Aggregation of β-amyloid (Aβ) is central to the pathogenesis of Alzheimer's disease (AD). Aβ aggregation produces amyloid assemblies, such as oligomers and fibrils. In contrast to non-toxic Aβ monomers, Aβ oligomers and fibrils can act directly as major toxic agents and indirectly as pools of the toxic entities, respectively. Thus, the detection of Aβ aggregates is of diagnostic interest and should benefit enhanced molecular understanding of AD. Among many molecular platforms, peptide-based ligands hold promise as Aβ probes due to their relative simplicity, ease of optimization and facile conjugation to other molecular contexts. In this regard, Aβ hydrophobic segments (critical in Aβ self-assembly) or variants thereof can serve as lead molecules for Aβ probe development. Unfortunately, the resulting peptides are either highly self-aggregation-prone or their probe potential has not been thoroughly examined. In the present study, we characterized a novel peptide ligand, KLVFWAK, which was created by simple point mutations of an Aβ hydrophobic segment (^{16}KLVFFAE^{22}). We found that KLVFWAK displayed low self-aggregation propensity and was preferentially bound to Aβ oligomers and fibrils relative to Aβ monomers. Interestingly, binding of KLVFWAK to Aβ aggregates occurred at a non-homologous Aβ segment (e.g., Aβ C-terminal domain) rather than the homologous ^{16}KLVFFAE^{22}. We also show that detection of Aβ aggregates during incubation of fresh Aβ was possible with KLVFWAK, further supporting KLVFWAK's high probe potential for Aβ aggregates. In short, this study presents creation of a non-self-aggregating peptide ligand for Aβ aggregates through simple point mutation of an Aβ-derived segment.

INTRODUCTION

Alzheimer's disease (AD) is a neurodegenerative disorder affecting ~5 million people in the USA.[1] It is characterized by cognitive impairment and neuropathological hallmarks comprising amyloid deposits and neuronal death in the brain.[2, 3] The principal constituent of amyloid deposits is a 40-42 amino acid peptide, β-amyloid (Aβ) (**Fig. 1**).[4] Aβ can self-aggregate spontaneously primarily due to hydrophobic interactions mediated by the hydrophobic central domain (HCD, L17-A21) and the hydrophobic C-terminus (I31-A40 or I31-A42) of Aβ.[5, 6] Aβ aggregation is a key molecular event responsible for AD pathology [2, 3] and begins with structurally disordered Aβ monomers,[7, 8] which self-assemble to β sheet structured oligomers [9-14] and fibrils.[15-17] In Aβ fibrils, Aβ HCDs and C-termini are oriented perpendicular to the long axis of fibrils to form parallel in-register β sheets.[15-17] No such parallel in-register β sheets are formed by Aβ oligomers where intermolecular arrangements of Aβ differ when compared to Aβ fibrils.[11-14] The primary toxic agents in AD are Aβ oligomers, which may disturb cell membranes, cause oxidative stress and inflammation, damage metabolism and perturb calcium homeostasis.[2, 3] It should also be noted that pre-formed Aβ fibrils may still be associated with neurotoxicity [2, 18, 19] by serving as either a catalytic surface for oligomerization[18] or a source of soluble oligomers by means of dissociation,[2, 20, 21] which is highly favorable at physiological Aβ concentrations.[22]

Facile profiling of Aβ aggregates (i.e., oligomers + fibrils) thus represents a significant step toward the development of early diagnostics and an enhanced understanding of a molecular basis of Aβ aggregation. Currently, the most widely used Aβ aggregate profiling methods are based on antibodies and antibody fragments with affinity for Aβ oligomers or fibrils.[23-25] Antibodies and antibody fragments must be well-folded in order for target binding but often suffer from insufficient conformational stability,[26] which limits their applications and further optimizations. Importantly, small peptide ligands may serve as an alternative tool for the recognition of Aβ aggregates and require no precise protein folding for binding to targets. Rational and combinatorial sequence variations as well as multi-valent displays are readily

available to further engineer peptide ligands for improved affinity and specificity. Peptide ligands can also be conjugated to other molecular scaffolds with precise control of spatial orientation, broadening the scope of sensing formats. Note that self-assembly of Aβ is mediated by its hydrophobic segments (e.g., ^{16}KLVFF^{20}), which can self-assemble.[27-29] Motivated by these findings, Aβ hydrophobic motifs have been exploited to create peptide ligands with affinity for Aβ.[29-34] Unfortunately, most Aβ-derived peptides display relatively low affinity for Aβ aggregates compared to Aβ monomers[29-32] and exhibit high self-aggregation propensity,[29-31, 35, 36] making Aβ-derived segments ill-suited to profile Aβ aggregates. Several modifications, such as terminal attachment of multiple charged residues, have proven effective for reduction of aggregation propensity of KLVFF-related sequences.[30, 37-41] However, potential of resulting peptides as a probe for Aβ aggregates and the related binding sites within Aβ have not been thoroughly examined.

In the study presented here, we report the development of a novel peptide ligand, KLVFWAK, which was derived from an Aβ fragment, ^{16}KLVFFAE^{22}. We found that KLVFWAK was highly resistant to self-aggregation but still able to bind to Aβ. Importantly, KLVFWAK was bound to Aβ aggregates (i.e., oligomers and fibrils) at least 10-times stronger than Aβ non-aggregates (i.e., monomers). Our competitive binding assays indicate that binding of KLVFWAK to Aβ occurred at a non-homologous Aβ segment (e.g., Aβ C-terminal domain) rather than the homologous ^{16}KLVFFAE^{22}. In addition, we show that formation of Aβ aggregates during incubation of fresh Aβ samples was readily detected by KLVFWAK. As discussed in this paper, KLVFWAK has high potential to serve as a lead ligand, which might readily evolve further for improved affinity and specificity. To the best of our knowledge, this is the first report to show that one can develop a non-self-aggregating peptide ligand for Aβ oligomers and Aβ fibrils through simple point mutation of Aβ-derived fragments.

RESULTS

Design of an Aβ-derived, non-self-aggregating peptide ligand, KLVFWAK

We have created an Aβ aggregate-specific, non-self-aggregating peptide ligand, KLVFWAK (**Fig. 1**), by engineering an Aβ fragment, ^{16}KLVFFAE^{22}, which is critical in Aβ self-assembly.[27-29] In this engineered peptide, the E22K mutation was introduced to increase solubility and to reduce self-aggregation propensity by enhancing self-electrostatic repulsion. The substituted tryptophan served for concentration determination. Importantly, KLVFWAK displays a substantial sequence similarity to Aβ hydrophobic central domain (HCD, i.e. ^{17}LVFFA^{21}). Thus, we initially thought that KLVFWAK was likely to bind to Aβ HCD, as this Aβ region is involved in homotypic interactions (between identical Aβ segments) during Aβ fibril formation.[14-16, 42] Another potential binding site within Aβ for KLVFWAK includes the Aβ C-terminus (^{31}IIGLMVGGVV^{40}), as this region is in contact with Aβ HCD in many Aβ oligomer structure models.[12-14] The presence of multiple copies of Aβ HCD and Aβ C-terminus in proximity within Aβ aggregates (i.e., oligomers and fibrils) would allow relatively strong binding of KLVFWAK to these Aβ aggregates compared to Aβ monomers. We also postulated that this short peptide could form no typical secondary structures (i.e., α helix and β sheet), making this peptide ligand difficult to bind to structurally disordered Aβ monomers due to a relatively high energetic cost needed for the binding.

A non-aggregating peptide ligand is usually preferred due to simplicity and ease of control. Desirably, KLVFWAK was found to be non-aggregating at 100 μM (i.e., a concentration 20-fold higher than that used for detection of Aβ aggregates in a fluorescent dot blot assay, see below) during overnight incubation, as determined by size exclusion chromatography (SEC) (**Fig. 2A**). The lack of significant aggregation was also confirmed by dynamic light scattering, where KLVFWAK solution at 100 μM scattered light no stronger than buffer during overnight incubation (i.e., 1.1 ± 0.3 kilo counts per second (kcps) for buffer and 1.2 ± 0.4 kcps for KLVFWAK solution). The size of KLVFWAK in solution could not be estimated using DLS due to the low scattering intensity. Circular dichroism (CD) spectrum of

KLVFWAK solution indicated the lack of typical secondary structures (i.e., α helix and β sheet) (**Fig. 2B**). A broad maximum at ~225 nm detected in this CD spectrum (**Fig. 2B**) is also consistent with the presence of local, if not global, polyproline-II helical structures within KLVFWAK.[43-46] More sophisticated characterizations will be required for further structural analysis.

Aβ binding of KLVFWAK

We examined binding of KLVFWAK to Aβ in monomeric, oligomeric and fibrillar forms using a fluorescent dot blot assay. For the examination, Aβ samples were prepared *in vitro* following the previously established protocols[6, 23, 47-50] (**Fig. 3**). As expected, of the three Aβ samples prepared *in vitro*, only Aβ oligomers were positive in a dot blot assay when probed with an antibody A11 (**Fig. 3A**), which recognizes a specific conformation of amyloid oligomers.[23] We also confirmed Aβ morphology in these samples using transmission electron microscopy (TEM): no notable Aβ aggregates were present in our Aβ monomer samples (**Fig. 3B**). In contrast, Aβ oligomer samples contained a mixture of globular aggregates with ~20 nm in diameter and protofibrillar species with ~200 nm in length, while a few μm-long mature fibrils were observed in Aβ fibril samples (**Fig. 3B**). In our Aβ monomer samples, structurally disordered low molecular weight (LMW) Aβ represented the dominant fraction as determined by native-PAGE (**Fig. S1**) and CD analysis (**Fig. S2**). The streaking bands corresponding to oligomeric Aβ rather than LMW Aβ were detected when our Aβ oligomer samples were run in native-PAGE (**Fig. S1**). Evidently, there existed a fraction of Aβ oligomers trapped in a well (**Fig. S1**). Collectively, this result is consistent with our previous finding: the major fraction (≥ ~80%) of our Aβ oligomer samples prepared using the same protocol was >70 kDa in size (corresponding to > 15-mer) with the minor fraction (≤ ~20%) consisting of Aβ monomers at 23 μM, as determined by SEC.[50] As expected, no band for Aβ fibril samples appeared in native-PAGE, as most Aβ fibrils were trapped in a well without entering a gel (**Fig. S1**).

We then blotted Aβ samples onto a membrane at 1 μg each. The membranes were subsequently incubated with 5 μM of KLVFWAK, which was labeled with fluorescein iso-thiocyanate (FITC) at the N-terminal α-amine (referred to as FITC-KLVFWAK) for easy identification. After multiple washing and rinsing of membranes to remove unbound peptides, FITC-KLVFWAK, which remained bound to Aβ, was detected and imaged based on fluorescence as described previously.[51] Our results indicate that FITC-KLVFWAK was selectively bound to Aβ aggregates (i.e., Aβ oligomers and Aβ fibrils), but not to Aβ monomers under our experimental condition (**Fig. 4A**). An additional assay demonstrates that ≥ 0.5 μg of Aβ aggregates were readily detectable by FITC-KLVFWAK under the experimental setup (**Fig. 4B**). In contrast, a fluorescence signal from FITC-KLVFWAK started to be noticeable at ≥ 5 μg of Aβ monomers (data not shown). It should however be noted that Aβ monomers can rapidly form Aβ oligomers at or below μM concentrations.[52, 53] Similarly, our Aβ monomer samples might contain non-negligible Aβ oligomers as shown in Fig. S1 and reported elsewhere,[54] particularly when a large mass of Aβ monomers was prepared. Thus, one may not exclude possibility that the aforementioned fluorescence signal with ≥ 5 μg of Aβ monomers might stem from Aβ oligomeric contaminants in samples. Overall, our peptide ligand exhibited at least 10 times stronger binding to Aβ aggregates compared to Aβ monomers.

To identify Aβ segments involved in binding of Aβ to KLVFWAK, we performed competitive binding assays between KLVFWAK and Aβ sequence-specific antibodies in a dot blot format where Aβ samples were blotted. The tested antibodies include 6E10, 4G8, anti-Aβ (22-35) and 9F1, recognizing Aβ M1-K16, Aβ L17-E22, Aβ E22-M35 and Aβ I32-V39, respectively.[34, 55-57] The panel of antibodies was carefully chosen for comprehensive evaluation of Aβ linear sequences involved in binding to KLVFWAK. Our competitive binding assay results indicate that binding of 9F1 to Aβ oligomers was significantly weakened with KLVFWAK present; in contrast, there was no such interference for 6E10, 4G8 and anti-AB (22-35) antibodies (**Fig. 5**, also see **Fig. S3** for a result from another independent experiment with

9F1). The implication of this result is that KLVFWAK was bound to the Aβ C-terminus in Aβ oligomers. We confirmed that Aβ oligomers remained oligomeric during competitive binding assays (**Fig. S4**). We observed no similar interference by KLVFWAK for binding of antibodies to Aβ fibrils (**Fig. 5**), despite the notable binding between FITC-KLVFWAK and Aβ fibrils in a fluorescent dot blot assay (**Fig. 4**). The results are consistent with the view that KLVFWAK might be bound to Aβ fibrils at non-consecutive Aβ residues originated from multiple Aβ molecules rather than consecutive amino acids in a single Aβ chain. Unlike Aβ oligomers and Aβ fibrils, no detectable binding to Aβ monomers of 9F1 occurred in the absence of KLVFWAK. The lack of binding might be due to intramolecular shielding of the Aβ C-terminus via its hydrophobic collapse occurring locally rather than globally or without forming any significant secondary structural elements in the Aβ monomeric state.[7, 58]

Aβ aggregation probed by KLVFWAK

Encouraged by the observed Aβ aggregate-specific recognition of FITC-KLVFWAK, we sought to examine Aβ aggregation using FITC-KLVFWAK. For this examination, we first prepared fresh Aβ solution at 50 μM and initiated Aβ aggregation by incubating the samples at 37 ^{o}C under a quiescent condition. Note that no FITC-KLVFWAK was added to these Aβ samples during incubation. Aliquots of Aβ samples were then withdrawn at several time points during incubation and subject to characterizations using Thioflavin T (ThT) fluorescence and TEM. ThT is a fluorescent dye recognizing amyloid β sheet structures found in Aβ oligomers and Aβ fibrils.[59] As reported elsewhere,[60, 61] ThT fluorescence of Aβ samples withdrawn during incubation showed a lag phase followed by a sigmoidal increase over time (**Figs. 6A and S5**). TEM images taken on the aliquoted Aβ samples further verified the progression of Aβ aggregation during incubation: Aβ samples lacked aggregates when freshly prepared (day 0) whereas significant Aβ aggregation took places to form a mixture of curved protofibrils and fibrils with a handful of globular oligomers (day 4), followed by emergence of dense fibril networks (day 9) (**Fig. 6B**). Aliquots

of the same Aβ samples were also blotted onto a membrane at 1 μg each for a fluorescent dot blot assay using FITC-KLVFWAK. In this assay, fluorescence signals were noticeable with Aβ samples incubating for 4-5 days or longer (**Fig. 6C**), verifying that FITC-KLVFWAK can detect Aβ aggregates in relatively complex samples obtained during Aβ aggregation. The lack of fluorescence signals from FITC-KLVFWAK with Aβ samples incubating less than 4 days indicates relatively low quantities of Aβ aggregates formed in the early stage of aggregation.

DISCUSSION

In this study, we explore the potential of an engineered Aβ fragment, KLVFWAK, as a peptide probe for Aβ aggregates. We show that KLVFWAK was preferentially bound to Aβ aggregates relative to Aβ monomers and could be used for probing of Aβ aggregates during Aβ incubation. Compared to many other KLVFF-related sequences, the lower aggregation propensity of KLVFWAK may facilitate reliable Aβ aggregate profiling by making interpretation of binding results straightforward. We also examined the related binding sites within Aβ aggregates and the results would benefit additional optimization of a peptide probe for improved affinity and specificity (see below).

Binding of KLVFWAK to structurally ordered Aβ oligomers and Aβ fibrils might be energetically favorable as suggested by computational studies of KLVFF binding to Aβ aggregates.[62] Conceivably, KLVFWAK binding to Aβ monomers can be relatively weak, as these Aβ forms are structurally disordered when compared to β sheet-structured Aβ aggregates (i.e., oligomers and fibrils).[63] Our competitive binding assays indicate that Aβ oligomers, but not Aβ fibrils, were bound to KLVFWAK via the Aβ C-terminus. The lack of involvement of the Aβ C-terminus in binding between Aβ fibrils and KLVFWAK might be due to low solvent accessibility of the Aβ domain in Aβ fibrillar states. However, our results indicate that the Aβ C-terminus was solvent-exposed in Aβ oligomers and fibrils to a sufficient

extent for binding to 9F1 (**Fig. 5**). The implication is that affinity of KLVFWAK to the Aβ C-terminus may at least in part depend on Aβ conformations, which are different between Aβ oligomers and fibrils.[11-16].

In contrast to the in-register, homotypic interaction present among Aβ ^{16}KLVFFAE^{22} residues on fibrils of the full length Aβ, no similar interaction was realized between KLVFWAK and the full-length Aβ (**Fig. 5**). This finding may point out the importance of Aβ residues flanking the Aβ HCD in arrangement of the in-register, β sheet-structures, as noted in computational docking of KLVFF to Aβ fibrils.[62] Our results shown in Figs. 4 and 5 are consistent with the view that KLVFWAK can bind to Aβ fibrils across multiple constituting Aβ molecules. This binding did not seem to be primarily mediated by the conjugated FITC, as we also detected binding to Aβ fibrils of KLVFWAK with biotin attached at the N-terminus in a dot blot study with horseradish peroxidase-conjugated streptavidin (data not shown). In Aβ fibrils, Aβ residues 1-15 are mostly structurally disordered.[15-17] On the other hand, the remaining Aβ residues form in-register β strand-loop-β strand structures.[15-17] These Aβ residues include those charged, such as D23 and K28 forming a buried salt-bridge in Aβ fibrils.[15, 16] On the other hand, Aβ E22 residues may form a negatively charged ladder on Aβ fibril surface[15, 16] and may serve as a potential binding site of positively charged KLVFWAK. Similarly, binding of a KLVFF-derived penta peptide was proposed to occur across multiple successive Aβ molecules constituting Aβ fibrils.[62, 64] In contrast, Aβ oligomers do not form in-register parallel β sheets [12-14] and thus a similar E22 ladder is unlikely to exist on Aβ oligomer surface. Instead, the E22 residue may salt-bridge with K28 and the side chain of D23 be buried by forming hydrogen bonds with the backbone amide groups of V24–K28 in non-fibrillar Aβ structures.[58] The relatively inefficient intermolecular electrostatic interaction may favor binding of KLVFWAK to the Aβ C-terminus, which is available for inter-molecular binding between Aβ oligomers and a KLVFF-related

sequence.[58] The two terminal lysine residues may improve KLVFWAK's heteromolecular interactions with Aβ C-terminus by disfavoring self-assembly of KLVFWAK.

The current detection limit of KLVFWAK for Aβ aggregates was determined to be 0.5 μg of Aβ. The physiological Aβ concentration is in the range of low nM in brain [22, 52, 65] and low pM in body fluids,[66, 67] requiring higher sensitivity for reliable *in vivo* or *ex vivo* detection using KLVFWAK. While the sensitivity of KLVFWAK appeared lower compared to currently available positron emission tomography (PET) ligands,[68, 69] the prototypical structure of our peptide ligand has high potential for enhanced sensitivity and desired specificity. For example, one may consider increasing Aβ aggregate-affinity by exploiting multivalency of KLVFWAK.[70] A multivalent display of peptide ligands has proven effective at increasing binding affinity substantially (e.g. > several orders of magnitudes) by elevating local ligand concentration and favoring multi-site binding to multimeric target analytes,[71, 72] such as Aβ aggregates. For the multivalent display, information on binding sites within Aβ may facilitate systematic improvement for functional affinity and specificity by optimizing intramolecular distance between multiple copies of KLVFWAK. For example, connection of two KLVFWAK motifs using molecular linkers spanning ~1-1.5 nm may enhance binding of these motifs to Aβ oligomers. This is because intermolecular distance between the Aβ binding sites, Aβ I32-V39 residues, is in this range in Aβ oligomers.[10, 12-14] One can vary the relative spatial position between KLVFWAK motifs in the multivalent peptide to explore both parallel and anti-parallel arrangements of Aβ binding sites. This exploration may lead to fine tuning of binding specificity, as β strands formed by Aβ I32-V39 residues are aligned differently between Aβ oligomers and Aβ fibrils.[11-16] Note that Aβ oligomers detectable by KLVFWAK may not necessarily represent all Aβ oligomers present. Thus, it would also be interesting to examine whether the nature of Aβ oligomer subpopulations detectable by peptide ligands can be altered by the multivalent display. This is because specific sets of a molecular linker and a spatial arrangement of KLVFWAK motifs might facilitate strong binding to Aβ oligomers in specific size and conformation.

While multivalent peptide ligands for Aβ were previously developed based on KLVFF, [31, 33, 70] their functional affinity and specificity were difficult to optimize systematically. This is in part due to high aggregation propensity of the peptide ligands and/or the lack of experimental determination of binding sites within Aβ. The specific chemical nature of PET ligands would also make similar systematic optimization of specificity and affinity difficult.[73] It should also be noted that the low aggregation propensity of peptide ligands would benefit the improvement of their binding affinity by increasing the number of binding sites available for Aβ. In short, our study presents promising potential for KLVFWAK as an alternative prototypical Aβ aggregate probe, which could readily be evolved for enhanced affinity and specificity.

EXPERIMENTAL

Materials

KLVFWAK was synthesized using solid-phase chemistry and purified using reverse-phase HPLC by Genscript (Piscataway, NJ, USA). KLVFWAK labeled with a fluorescent dye, fluorescein iso-thiocyanate (FITC) at the N-terminal α-amine (referred to as FITC-KLVFWAK), was similarly produced by Genscript. Lyophilized β-amyloid (Aβ) containing 40 residues (D1-V40) was purchased from the ERI Amyloid Laboratory (Oxford, CT, USA). Aβ sequence-specific antibodies, 6E10 and 4G8 were purchased from Covance (Princeton, NJ, USA). Other Aβ sequence-specific antibodies, anti-Aβ (22-35) and 9F1, were obtained from Sigma Aldrich (St. Louis, MO, USA) and Enzo Life Sciences (Farmingdale, NY, USA), respectively. A precision column prepacked with Superdex 75 was purchased from GE Healthcare (Piscataway, NJ, USA). All other chemicals were purchased from Fisher Scientific (Pittsburg, PA, USA), unless otherwise stated.

KLVFWAK sample preparation

Lyophilized KLVFWAK was dissolved at 1.12 mM in phosphate-buffered saline with azide (PBSA, 1X PBSA contains 20 mM Na_2HPO_4/NaH_2PO_4, 150 mM NaCl, and 0.02% (w/v) NaN_3 at pH 7.4). The peptide solution was then filtered with Millipore 0.45 μm syringe filters (EMD Millipore, Billerica, MA, USA). FITC-KLVFWAK solutions were prepared similarly in PBSA at an initial concentration of 100 μM.

Aβ sample preparation

Aβ samples were prepared according to established protocols where lyophilized Aβ powders were pre-treated with hexafluoroisopropanol (HFIP) at 1 mg of Aβ per 500 μl of HFIP [23, 47, 48] and then vacuum-dried. The HFIP-treated, re-dried samples were then stored at -80˚C until preparation was needed. Aβ samples were prepared in glass vials. The following protocols were previously shown to successfully produce Aβ monomer, Aβ oligomer and Aβ fibril samples.[6, 49, 50]

For preparation of Aβ monomer samples, 20 mM NaOH was first added to the HFIP-treated, re-dried Aβ for 20 min at a peptide concentration of 650 μM in solution. Aβ solution in NaOH was kept on ice throughout this procedure. This NaOH treatment was found to be effective for disrupting initial structures of Aβ and dissociating pre-existing aggregates to their unfolded monomeric states.[48, 74] Then, cold deionized water, 10X PBSA, and 30X PBA (i.e., PBSA without NaCl) were added to the sample for a final buffer concentration of 80 mM Na_2HPO_4/NaH_2PO_4, 150 mM NaCl and 0.02% (w/v) NaN_3 at pH 7.6. The sample was then filtered with Millipore 0.45 μm syringe filters. The concentrations of the filtered Aβ solutions were measured by UV at 280 nm with correction for light scattering effects.[75] Aβ concentration of the sample was then adjusted to 230 μM or 50 μM by adding buffer. Aβ monomer samples were freshly prepared each time and used immediately.

For preparation of Aβ oligomer samples, the HFIP-treated, re-dried Aβ was dissolved in dimethyl sulfoxide (DMSO) at a peptide concentration of ~ 5 mM for at least 20 min. Deionized water and 10X PBSA were then added for a final concentration of 20 mM Na_2HPO_4/NaH_2PO_4, 150 mM NaCl, and .02% (w/v) NaN_3 at pH 7.2, and a final Aβ concentration of 230 μM. Aβ samples were subsequently incubated at 37˚C for 3 days under a quiescent condition. Supernatants were then collected after centrifugation and Aβ concentrations subsequently measured using UV at 280 nm as described above.

Fibril samples were prepared by dissolution of the HFIP-treated, re-dried Aβ in DMSO at ~ 5 mM peptide concentration for at least 20 min, followed by dilution into PBSA at a peptide concentration of 230 μM. The Aβ samples were then incubated for ~4-6 weeks at 37 ^{o}C with continuous stirring by a magnetic stir bar at 400 rpm. After incubation, samples were centrifuged for 15 min to discard soluble fractions. Insoluble pellets were subsequently washed multiple times with PBSA and resuspended with the same buffer. Soluble Aβ concentrations were measured using UV at 280 nm during each washing, rinsing and centrifugation, and the Aβ fibril concentrations were then back-calculated.

Time-course Aβ aggregation

Aβ samples used for time-course aggregation analyses were prepared by initially dissolving the HFIP-treated, re-dried Aβ in DMSO for 20 min. The initial DMSO dissolution was used to ensure that Aβ initially existed as monomers, as reported elsewhere.[76] After subsequent dilution to PBSA at a peptide concentration of 50 μM, the Aβ samples were further incubated at 37 °C under a quiescent condition to initiate aggregation. Aliquots of Aβ samples were removed at different time points during the aggregation process and subject to characterizations using Thioflavin T fluorescence, Transmission Electron Microscopy and fluorescent dot blot assays with FITC-KLVFWAK.

Thioflavin T (ThT) fluorescence

Twenty μL of Aβ solutions were mixed with 5 μL of ThT solution at 0.1 mM and 175 μL of PBSA. The ThT fluorescence of the samples was then immediately measured on a Photon Technology QuantaMaster QM-4 spectrofluorometer (Photon Technology International, Edison, NJ, USA). The excitation wavelength was 440 nm, and emission was monitored at 487 nm.

Dot blot assays

One μg, unless otherwise mentioned, of peptides in solution was applied to a nitrocellulose membrane and allowed to air dry at room temperature for 15 min. Blocking, washing, incubation with primary and alkaline phosphatase-conjugated secondary antibodies, and chemiluminescent development were performed according to the manufacturer's protocols. A fluorescence dot blot assay using 5 μM FITC-KLVFWAK as a probe was performed similarly, except for the omittance of secondary antibody incubation. In this case, detection was achieved using the Molecular Dynamics Storm 840 molecular phosphorimager system housed at the NYU Chemistry Department Shared Instrumentation Facilities Center or the NYU Langone Medical Center. For competitive binding assays, several Aβ sequence-specific antibodies were used as primary antibodies including 6E10, 4G8, anti-Aβ (22-35) and 9F1, which recognize Aβ M1-K16, Aβ L17-E22, Aβ E22-M35 and Aβ I32-V39, respectively.[34, 55-57] If necessary, membranes were incubated in stripping buffer (0.2 M Glycine, 3.5 mM SDS, 1% (v/v) Tween-20, pH 2.2) overnight to remove bound sequence-specific antibodies, followed by washing, rinsing, and a subsequent blotting procedure with A11.

Transmission electron microscopy (TEM)

The aliquots (5 μL) of a sample were pipetted on copper grids and then negatively stained with 1% uranyl acetate in deionized water for 15 min. The samples were imaged on a Philips CM12 Transmission Electron Microscope (FEI Corp. Hillsboro, OR, USA) at 120 kV with a 4 k × 2.67 k GATAN digital

camera located at the NYU Langone Medical Center.

Size exclusion chromatography (SEC)

Aggregation of KLVFWAK in solution was analyzed with size exclusion chromatography (SEC) using a precision column prepacked with Superdex 75 (separation range from 3 to 70 kDa, GE healthcare) on a GE FPLC system, as described previously.[51, 77] Briefly, the mobile phase flow rate was set at 0.1 ml/min and elution peaks were detected by UV absorbance at 280 nm. The mobile phase buffer was PBSA used for preparation of peptide samples. The column was calibrated using the following proteins as molecular weight standards: ribonuclease A (13.7 kDa), carbonic anhydrase (29 kDa), ovalalbumin (44kDa) and conalbumin (75kDa) (GE Healthcare).

Laser Light Scattering

Aggregation of KLVFWAK in solution was also monitored by laser light scattering using the Zetasizer Nano-S system (Malvern Instruments Ltd., Malvern, UK). KLVFWAK samples were placed in quartz cuvettes and intensities of scattered light at 633 nm were then measured at 90° relative to the incident light at the same wavelength.

Circular dichroism (CD) spectroscopy

Secondary structures of proteins in solution were determined by CD. Spectra were collected on a Jasco J-815 spectropolarimeter in the far-UV range with a 0.1 cm pathlength cuvette. The spectrum of the background (buffer only) was subtracted from the sample spectrum.

Native-PAGE

Aβ samples were resolved by native polyacrylamide gel electrophoresis (native-PAGE), which was performed with an XCell SureLock Novex Mini-Cell electrophoresis system purchased from Life technologies (Carlsbad, CA, USA) under a non-denaturing condition. For native-PAGE, NativePAGE 4-

16% Bis-Tris Gel (Life technologies) was used and 8 μg of a sample was loaded into a well without any additional sample pretreatment.

ACKNOWLEDGMENTS

The authors are grateful for supports from the National Science Foundation (CBET- 1159699).

Electronic Supplementary Information (ESI) available: [Figs. S1, S2, S3, S4 and S5].

REFERENCES

1. L. E. Hebert, J. Weuve, P. A. Scherr, and D. A. Evans, *Neurology*, 2013, **80**, 1778-1783.
2. C. Haass, and D. J. Selkoe, *Nat. Rev. Mol. Cell. Biol.*, 2007, **8**, 101-112.
3. A. Aguzzi, and T. O'Connor, *Nat. Rev. Drug. Discov.*, 2010, **9**, 237-248.
4. J. Kang, H. G. Lemaire, A. Unterbeck, J. M. Salbaum, C. L. Masters, K. H. Grzeschik, G. Multhaup, K. Beyreuther, and B. Muller-Hill, *Nature*, 1987, **325**, 733-736.
5. R. Liu, C. McAllister, Y. Lyubchenko, and M. R. Sierks, *J. Neurosci. Res.*, 2004, **75**, 162-171.
6. Y. Hu, H. Zheng, B. Su, M. Hernandez, and J. R. Kim, *Biochim. Biophys. Acta*, 2012, **1824**, 1069-1079.
7. S. Zhang, K. Iwata, M. J. Lachenmann, J. W. Peng, S. Li, E. R. Stimson, Y. Lu, A. M. Felix, J. E. Maggio, and J. P. Lee, *J. Struct. Biol.*, 2000, **130**, 130-141.
8. N. D. Lazo, M. A. Grant, M. C. Condron, A. C. Rigby, and D. B. Teplow, *Protein Sci.*, 2005, **14**, 1581-1596.
9. S. Chimon, M. A. Shaibat, C. R. Jones, D. C. Calero, B. Aizezi, and Y. Ishii, *Nat. Struct. Mol. Biol.*, 2007, **14**, 1157-1164.
10. J. C. Stroud, C. Liu, P. K. Teng, and D. Eisenberg, *Proc. Natl. Acad. Sci. U. S. A.*, 2012, **109**, 7717-7722.

11. L. Yu, R. Edalji, J. E. Harlan, T. F. Holzman, A. P. Lopez, B. Labkovsky, H. Hillen, S. Barghorn, U. Ebert, P. L. Richardson, L. Miesbauer, L. Solomon, D. Bartley, K. Walter, R. W. Johnson, P. J. Hajduk, and E. T. Olejniczak, *Biochemistry*, 2009, **48**, 1870-1877.

12. L. Gu, C. Liu, J. C. Stroud, S. Ngo, L. Jiang, and Z. Guo, *J. Biol. Chem.*, 2014, **289**, 27300-27313.

13. W. M. Tay, D. Huang, T. L. Rosenberry, and A. K. Paravastu, *J. Mol. Biol.*, 2013, **425**, 2494-2508.

14. M. Ahmed, J. Davis, D. Aucoin, T. Sato, S. Ahuja, S. Aimoto, J. I. Elliott, W. E. Van Nostrand, and S. O. Smith, *Nat. Struct. Mol. Biol.*, 2010, **17**, 561-567.

15. A. T. Petkova, Y. Ishii, J. J. Balbach, O. N. Antzutkin, R. D. Leapman, F. Delaglio, and R. Tycko, *Proc. Natl. Acad. Sci. U. S. A.*, 2002, **99**, 16742-16747.

16. T. Luhrs, C. Ritter, M. Adrian, D. Riek-Loher, B. Bohrmann, H. Dobeli, D. Schubert, and R. Riek, *Proc. Natl. Acad. Sci. U. S. A.*, 2005, **102**, 17342-17347.

17. H. A. Scheidt, I. Morgado, S. Rothemund, and D. Huster, *J. Biol. Chem.*, 2012, **287**, 2017-2021.

18. S. I. Cohen, P. Arosio, J. Presto, F. R. Kurudenkandy, H. Biverstal, L. Dolfe, C. Dunning, X. Yang, B. Frohm, M. Vendruscolo, J. Johansson, C. M. Dobson, A. Fisahn, T. P. Knowles, and S. Linse, *Nat. Struct. Mol. Biol.*, 2015, **22**, 207-213.

19. K. Matsuzaki, *Acc. Chem. Res.*, 2014, **47**, 2397-2404.

20. P. Narayan, A. Orte, R. W. Clarke, B. Bolognesi, S. Hook, K. A. Ganzinger, S. Meehan, M. R. Wilson, C. M. Dobson, and D. Klenerman, *Nat. Struct. Mol. Biol.*, 2012, **19**, 79-83.

21. L. Sanchez, S. Madurga, T. Pukala, M. Vilaseca, C. Lopez-Iglesias, C. V. Robinson, E. Giralt, and N. Carulla, *J. Am. Chem. Soc.*, 2011, **133**, 6505-6508.

22. P. Sengupta, K. Garai, B. Sahoo, Y. Shi, D. J. Callaway, and S. Maiti, *Biochemistry*, 2003, **42**, 10506-10513.

23. R. Kayed, E. Head, J. L. Thompson, T. M. McIntire, S. C. Milton, C. W. Cotman, and C. G. Glabe, *Science*, 2003, **300**, 486-489.

24. S. Kasturirangan, T. Reasoner, P. Schulz, S. Boddapati, S. Emadi, J. Valla, and M. R. Sierks, *Biotechnol. Prog.*, 2013, **29**, 463-471.

25. I. Morgado, K. Wieligmann, M. Bereza, R. Ronicke, K. Meinhardt, K. Annamalai, M. Baumann, J. Wacker, P. Hortschansky, M. Malesevic, C. Parthier, C. Mawrin, C. Schiene-Fischer, K. G. Reymann, M. T. Stubbs, J. Balbach, M. Gorlach, U. Horn, and M. Fandrich, *Proc. Natl. Acad. Sci. U. S. A.*, 2012, **109**, 12503-12508.

26. R. Rouet, D. Lowe, and D. Christ, *FEBS Lett.*, 2014, **588**, 269-277.

27. T. Christopeit, P. Hortschansky, V. Schroeckh, K. Guhrs, G. Zandomeneghi, and M. Fandrich, *Protein Sci.*, 2005, **14**, 2125-2131.

28. J. J. Balbach, Y. Ishii, O. N. Antzutkin, R. D. Leapman, N. W. Rizzo, F. Dyda, J. Reed, and R. Tycko, *Biochemistry*, 2000, **39**, 13748-13759.

29. L. O. Tjernberg, J. Naslund, F. Lindqvist, J. Johansson, A. R. Karlstrom, J. Thyberg, L. Terenius, and C. Nordstedt, *J. Biol. Chem.*, 1996, **271**, 8545-8548.

30. C. W. Cairo, A. Strzelec, R. M. Murphy, and L. L. Kiessling, *Biochemistry*, 2002, **41**, 8620-8629.

31. A. A. Reinke, P. M. Ung, J. J. Quintero, H. A. Carlson, and J. E. Gestwicki, *J. Am. Chem. Soc.*, 2010, **132**, 17655-17657.

32. B. P. Orner, L. Liu, R. M. Murphy, and L. L. Kiessling, *J. Am. Chem. Soc.*, 2006, **128**, 11882-11889.

33. G. Zhang, M. J. Leibowitz, P. J. Sinko, and S. Stein, *Bioconjug. Chem.*, 2003, **14**, 86-92.

34. J. M. Perchiacca, A. R. Ladiwala, M. Bhattacharya, and P. M. Tessier, *Proc. Natl. Acad. Sci. U. S. A.*, 2012, **109**, 84-89.

35. T. Arai, T. Araya, D. Sasaki, A. Taniguchi, T. Sato, Y. Sohma, and M. Kanai, *Angew. Chem. Int. Ed. Engl.*, 2014, **53**, 8236-8239.

36. V. Castelletto, G. Cheng, and I. W. Hamley, *Chem. Commun. (Camb)*, 2011, **47**, 12470-12472.

37. T. Arai, D. Sasaki, T. Araya, T. Sato, Y. Sohma, and M. Kanai, *Chembiochem*, 2014, **15**, 2577-2583.

38. M. A. Etienne, J. P. Aucoin, Y. Fu, R. L. McCarley, and R. P. Hammer, *J. Am. Chem. Soc.*, 2006, **128**, 3522-3523.

39. J. R. Kim, T. J. Gibson, and R. M. Murphy, *Biotechnol. Prog.*, 2006, **22**, 605-608.

40. C. K. Bett, W. K. Serem, K. R. Fontenot, R. P. Hammer, and J. C. Garno, *ACS Chem. Neurosci.*, 2010, **1**, 661-678.

41. B. M. Austen, K. E. Paleologou, S. A. Ali, M. M. Qureshi, D. Allsop, and O. M. El-Agnaf, *Biochemistry*, 2008, **47**, 1984-1992.

42. J. P. Colletier, A. Laganowsky, M. Landau, M. L. Zhao, A. B. Soriaga, L. Goldschmidt, D. Flot, D. Cascio, M. R. Sawaya, and D. Eisenberg, *Proc. Natl. Acad. Sci. U. S. A.*, 2011, **108**, 16938-16943.

43. F. Eker, K. Griebenow, and R. Schweitzer-Stenner, *J. Am. Chem. Soc.*, 2003, **125**, 8178-8185.

44. E. W. Ronish, and S. Krimm, *Biopolymers*, 1974, **13**, 1635-1651.

45. A. L. Rucker, and T. P. Creamer, *Protein Sci.*, 2002, **11**, 980-985.

46. M. A. Kelly, B. W. Chellgren, A. L. Rucker, J. M. Troutman, M. G. Fried, A. F. Miller, and T. P. Creamer, *Biochemistry*, 2001, **40**, 14376-14383.

47. K. N. Dahlgren, A. M. Manelli, W. B. Stine, Jr., L. K. Baker, G. A. Krafft, and M. J. LaDu, *J. Biol. Chem.*, 2002, **277**, 32046-32053.

48. D. B. Teplow, *Methods Enzymol.*, 2006, **413**, 20-33.

49. Y. Hu, B. Su, H. Zheng, and J. R. Kim, *Mol. Biosyst.*, 2012, **8**, 2741-2752.

50. Y. Hu, B. Su, C. S. Kim, M. Hernandez, A. Rostagno, J. Ghiso, and J. R. Kim, *Chembiochem*, 2010, **11**, 2409-2418.

51. M. Hernandez, Y. Hu, and J. R. Kim, *Chem. Commun. (Camb)*, 2013, **49**, 10712-10714.

52. H. LeVine, 3rd, *Anal. Biochem.*, 2004, **335**, 81-90.

53. S. Nag, B. Sarkar, A. Bandyopadhyay, B. Sahoo, V. K. Sreenivasan, M. Kombrabail, C. Muralidharan, and S. Maiti, *J. Biol. Chem.*, 2011, **286**, 13827-13833.

54. M. M. Pallitto, and R. M. Murphy, *Biophys. J.*, 2001, **81**, 1805-1822.

55. X. Li, X. Zhang, A. R. Ladiwala, D. Du, J. K. Yadav, P. M. Tessier, P. E. Wright, J. W. Kelly, and J. N. Buxbaum, *J. Neurosci.*, 2013, **33**, 19423-19433.

56. J. A. Irwin, H. Edward Wong, and I. Kwon, *Anal. Biochem.*, 2015, **470**, 61-70.

57. S. K. Singh, R. Gaur, A. Kumar, R. Fatima, L. Mishra, and S. Srikrishna, *Neurotox. Res.*, 2014, **26**, 331-350.

58. D. J. Rosenman, C. R. Connors, W. Chen, C. Wang, and A. E. Garcia, *J. Mol. Biol.*, 2013, **425**, 3338-3359.

59. H. LeVine, 3rd, *Methods Enzymol.*, 1999, **309**, 274-284.

60. A. D. Williams, E. Portelius, I. Kheterpal, J. T. Guo, K. D. Cook, Y. Xu, and R. Wetzel, *J. Mol. Biol.*, 2004, **335**, 833-842.

61. Y. Yoshiike, D. H. Chui, T. Akagi, N. Tanaka, and A. Takashima, *J. Biol. Chem.*, 2003, **278**, 23648-23655.

62. M. H. Viet, S. T. Ngo, N. S. Lam, and M. S. Li, *J. Phys. Chem. B*, 2011, **115**, 7433-7446.

63. A. Zhang, W. Qi, T. A. Good, and E. J. Fernandez, *Biophys. J.*, 2009, **96**, 1091-1104.

64. Z. Chen, G. Krause, and B. Reif, *J. Mol. Biol.*, 2005, **354**, 760-776.

65. W. A. van Gool, M. A. Kuiper, G. J. Walstra, E. C. Wolters, and P. A. Bolhuis, *Ann. Neurol.*, 1995, **37**, 277-279.

66. A. Leinenbach, J. Pannee, T. Dulffer, A. Huber, T. Bittner, U. Andreasson, J. Gobom, H. Zetterberg, U. Kobold, E. Portelius, and K. Blennow, *Clin. Chem.*, 2014, **60**, 987-994.

67. V. De Riva, E. Galloni, M. Marcon, L. Di Dionisio, C. Deluca, L. Meligrana, A. Bolner, and F. Perini, *Clin. Lab.*, 2014, **60**, 629-634.

68. L. M. Shaw, H. Vanderstichele, M. Knapik-Czajka, C. M. Clark, P. S. Aisen, R. C. Petersen, K. Blennow, H. Soares, A. Simon, P. Lewczuk, R. Dean, E. Siemers, W. Potter, V. M. Lee, and J. Q. Trojanowski, *Ann. Neurol.*, 2009, **65**, 403-413.

69. D. Brockschnieder, H. Schmitt-Willich, T. Heinrich, A. Varrone, B. Gulyas, M. Toth, J. Andersson, U. Boemer, S. Krause, M. Friebe, L. Dinkelborg, C. Halldin, and T. Dyrks, *J. Nucl. Med.*, 2012, **53**, 1794-1801.

70. S. M. Chafekar, H. Malda, M. Merkx, E. W. Meijer, D. Viertl, H. A. Lashuel, F. Baas, and W. Scheper, *Chembiochem*, 2007, **8**, 1857-1864.

71. J. E. Gestwicki, and L. L. Kiessling, *Nature*, 2002, **415**, 81-84.

72. C. Fasting, C. A. Schalley, M. Weber, O. Seitz, S. Hecht, B. Koksch, J. Dernedde, C. Graf, E. W. Knapp, and R. Haag, *Angew. Chem. Int. Ed. Engl.*, 2012, **51**, 10472-10498.

73. D. D. Nolting, M. L. Nickels, N. Guo, and W. Pham, *Am. J. Nucl. Med. Mol. Imaging*, 2012, **2**, 273-306.

74. M. G. Zagorski, J. Yang, H. Shao, K. Ma, H. Zeng, and A. Hong, *Methods Enzymol.*, 1999, **309**, 189-204.

75. H. Mach, D. B. Volkin, C. J. Burke, and C. R. Middaugh, *Methods Mol. Biol.*, 1995, **40**, 91-114.

76. J. J. Kremer, M. M. Pallitto, D. J. Sklansky, and R. M. Murphy, *Biochemistry*, 2000, **39**, 10309-10318.

77. M. Hernandez, S. Golbert, L. G. Zhang, and J. R. Kim, *Chembiochem*, 2011, **12**, 2630-2639.

FIGURE LEGENDS

Fig. 1 An amino acid sequence of Aβ containing 40 amino acids along with an engineered peptide ligand for Aβ aggregates, KLVFWAK. The Aβ sequence, where KLVFWAK was derived, is colored in red.

Fig. 2 (A) Size Exclusion Chromatogram (SEC) of KLVFWAK at 100 μM obtained immediately after preparation (red) and after 1 day incubation (blue) at room temperature. A column volume of Superdex 75 (separation range from 3 to 70 kDa) corresponds to ~2.4 ml at which small molecules less than 3 kDa in size elute. The results shown here demonstrate the lack of significant aggregation of KLVFWAK under our experimental setup. **(B)** Circular Dichroism (CD) of KLVFWAK at 100 μM (red) and 300 μM (blue) measured at room temperature.

Fig. 3 (A) Dot blot assays and **(B)** morphologies of Aβ monomers (M), Aβ oligomers (O) and Aβ fibrils (F) prepared *in vitro*. In (A), an antibody A11 recognizing specific conformations of Aβ oligomers was used. In (B), scale bars : 200 nm.

Fig. 4 Fluorescent dot blot assays using FITC-KLVFWAK of Aβ monomers (M), Aβ oligomers (O) and Aβ fibrils (F) blotted onto a membrane at **(A)** 1 μg each and **(B)** 0.05 – 1 μg each. In (A), an image from bright field illumination is shown in the bottom panel.

Fig. 5 Dot blot assays of Aβ samples (monomers (M), oligomers (O) and fibrils (F) in the first, second and third columns, respectively, in each panel) in the absence (N, the first row in each panel) and presence (Y, the second row in each panel) of KLVFWAK using antibodies, 6E10, 4G8, Anti-Aβ (22-35) and 9F1. The molar concentration ratio of [Aβ]/[KLVFWAK] = 1:10 for the second row of each panel.

Fig. 6 Time course aggregation of Aβ at 50 μM monitored by **(A)** ThT fluorescence, **(B)** TEM and **(C)** fluorescent dot blot assays with FITC-KLVFWAK. Aβ samples were incubated at 37 ^{o}C under a quiescent condition and aliquots withdrawn at designated time points during incubation for subsequent characterizations. In (B), scale bars : 200 nm.

Fig. 1

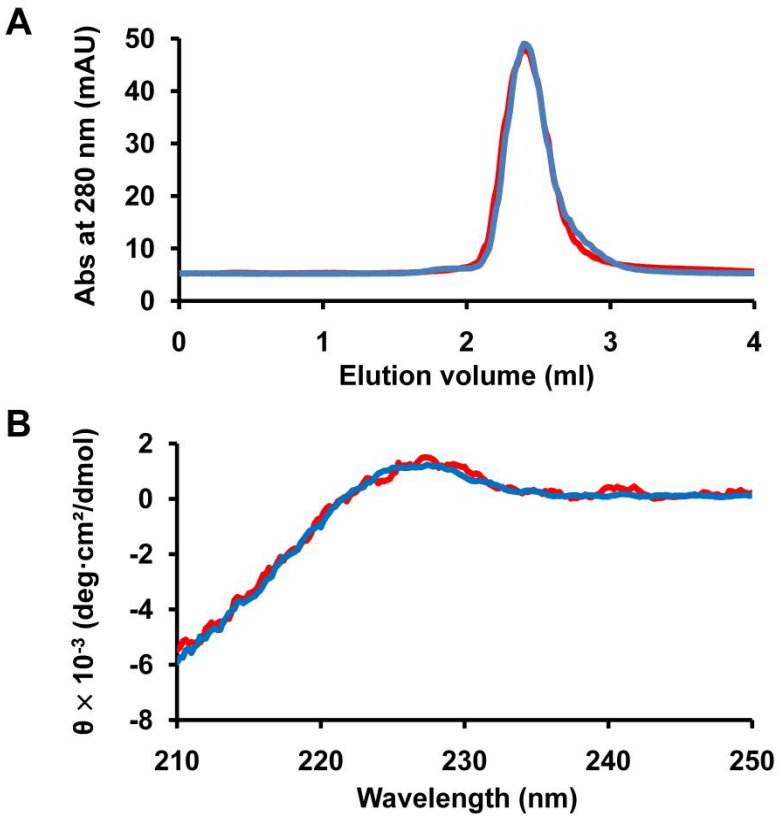

Fig. 2

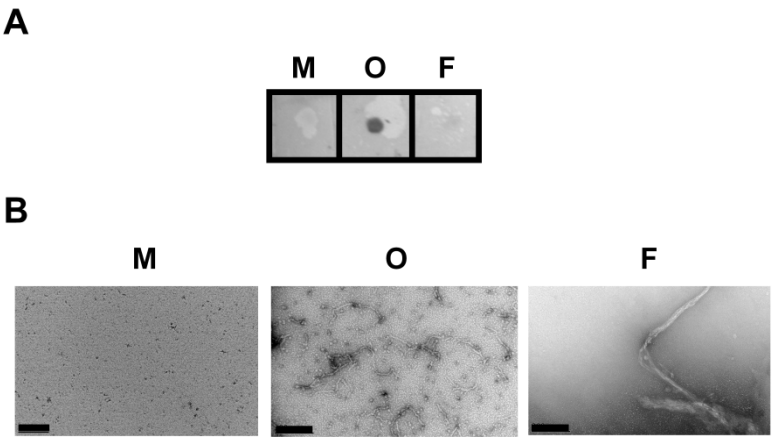

Fig. 3

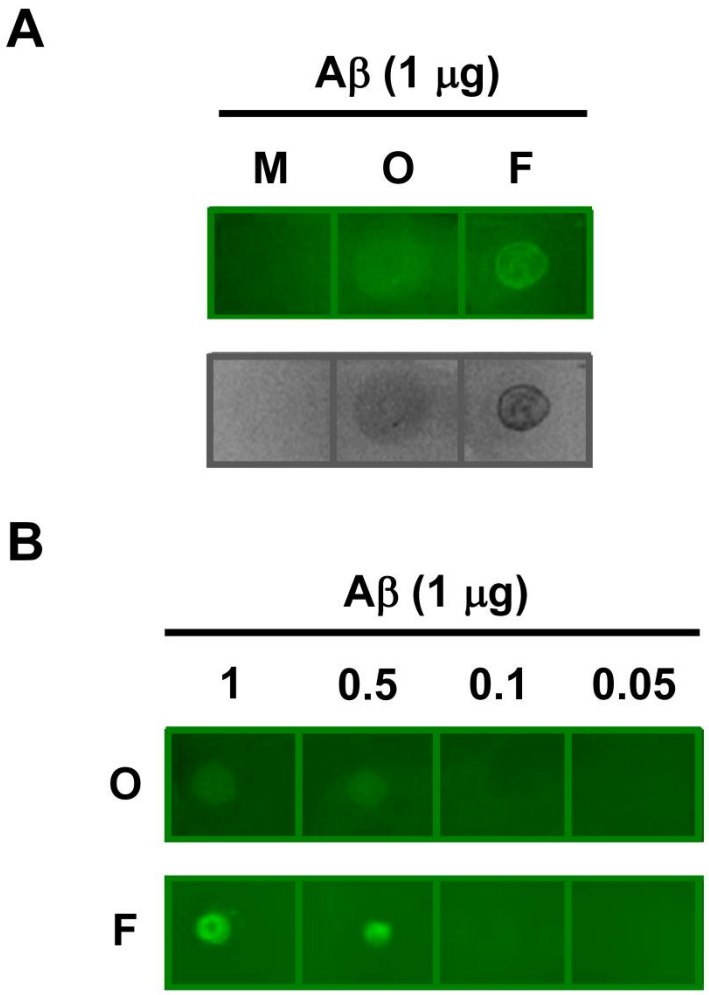

Fig. 4

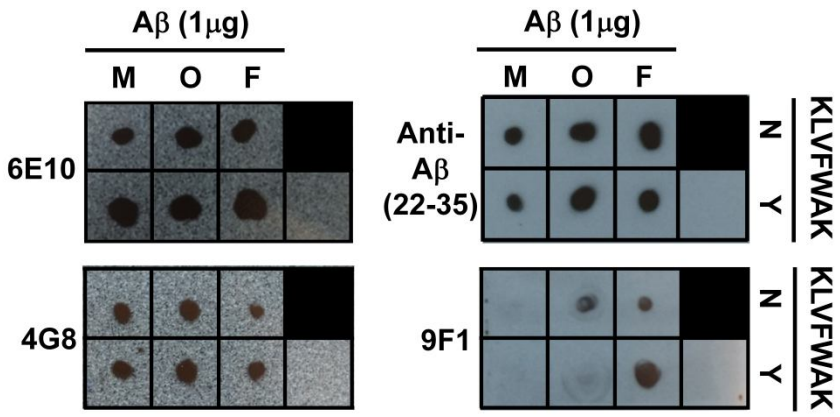

Fig. 5

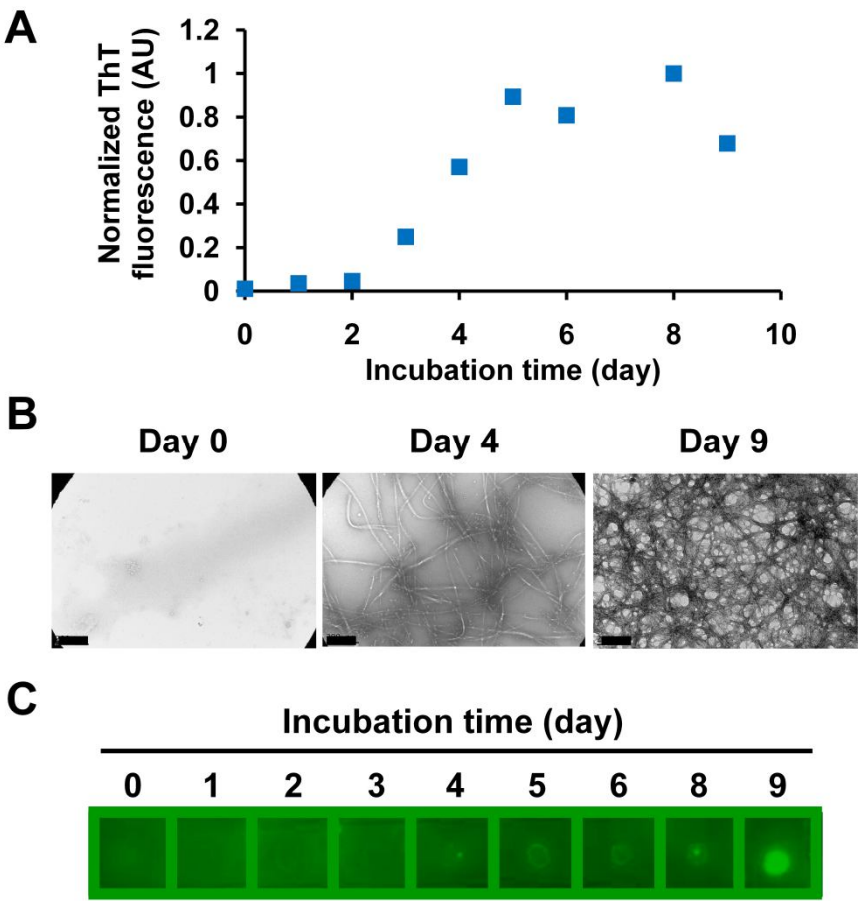

Fig. 6